43. PHYSICAL PROPERTIES OF BASALTS FROM DEEP SEA DRILLING PROJECT HOLE 504B, COSTA RICA RIFT[1]

Shun-ichiro Karato,[2] Ocean Research Institute, University of Tokyo, Minamidai, Nakano, Tokyo 164, Japan

ABSTRACT

A detailed study of physical properties was made on core samples from Deep Sea Drilling Project Hole 504B. The measured properties are density, porosity, sonic velocity, electrical resistivity, and fluid permeability. Basalts from this young oceanic crust have higher density and sonic velocity than the average DSDP basalts. Porosity (and temperature) dependences of physical properties are given by

$$V = V_0 - a\phi$$

$$\varrho = \varrho_0 \exp(E^*/RT)\, \phi^{-q}$$

$$k = k_0' \phi^{2q-1}$$

where V is the sonic velocity (km/s), $V_0 = 6.45$ (km/s), $a = 0.111$ (km/s %), ϕ is the porosity (%), ϱ is the electrical resistivity (ohm m), $\varrho_0 = 0.002$ (ohm m), $E^* = 2.7$ (Kcal/mol) for fresh basalts, RT has its usual meaning, $q = 1.67 \pm 0.27$, k is the permeability, $k_0' = (1 \sim 10) \times 10^{-12}$ (cm^2). Porosity distribution in the crust in this area is estimated by combining the seismic velocity distribution and velocity–porosity relation. Because of the rapid decrease in porosity with depth, resistivity increases and permeability decreases rapidly with depth. The decreasing rate of permeability with increasing depth is approximately given by $k(\text{cm}^2) = 2 \times 10^{-10} \exp(-z\ (\text{km})/0.3)$.

INTRODUCTION

Hole 504B, south of the Costa Rica Rift, provides a good opportunity for studying the physical state of the young oceanic crust, because of the deep basement penetration (562 m) on the one hand, and the successful logging (Cann and Von Herzen, this volume), on the other.

A comprehensive study of physical properties, including density, porosity, sonic (compressional-wave) velocity, electrical resistivity, and fluid permeability was made for a large collection of basalts cored from this hole. This study, combined with logging data, will provide a basis for understanding this young oceanic crust.

Because the velocity of seismic waves is the major source of information about the deep structure of the oceanic crust (e.g., Ewing and Houtz, 1979), the importance of its study is well recognized, and numerous works have been done on the sonic velocity of oceanic basalts (e.g., Christensen and Salisbury, 1975). These studies have confirmed the importance of pore space on the velocity structure of oceanic crust.

The recent discovery that hydrothermal circulation occurs in young oceanic crust (e.g., Lister, 1972; Williams et al., 1974; Anderson et al., 1977) stresses the importance of the nature of pore structure in the oceanic crust. Although the difference in dimension between hand specimen and the oceanic crust may be significant, laboratory study of the nature of porosity in oceanic basalts may provide a basis for understanding the pore structure in oceanic crust.

The electrical resistivity and the fluid permeability of fluid-saturated rocks are closely related to the nature of pores and could give valuable information about the shape and dimension of pores (Shankland and Waff, 1975; Brace, 1977); however, only a little work has been done on the electrical resistivity and fluid permeability of oceanic basalts. In particular, the measurement of fluid permeability of oceanic basalts has been made only recently (Johnson, 1979). This report is probably the first comprehensive study of fluid permeability of young oceanic basalts.

Since the physical properties studied here are sensitive to water content, all the measurements except porosity were made on sea-water-saturated samples with 2.5-cm diameter and 2- to 5-cm length. The results of all the measurements and their mean values are given in Tables 1 and 2 respectively. Histograms of physical properties are given in Figure 1.

GRAVIMETRIC MEASUREMENTS

The wet-bulk density of basalts was determined by weighing samples first in air to determine the mass and then suspended in water to determine the volume. Water content was determined by weighing samples first saturated with sea water, then after drying at 110°C for 24 hours. Porosity and grain density were calculated from the wet-bulk density and water content. The accuracy of each measurement was about 0.001 g, and the reproducibility was about 0.005 g; thus, the experimental error of density is about 0.1% and that of porosity about 1%.

[1] Cann, J. R., Langseth, M. G., Honnorez, J., Von Herzen, R. P., White, S. M., et al., *Init. Repts. DSDP*, 69: Washington (U.S. Govt. Printing Office).

[2] Present address: Research School of Earth Sciences, The Australian National University, P.O. Box 4, Canberra 2600, Australia.

Table 1. Physical properties of basalts from Hole 504B.

Sample (interval in cm)	Wet-Bulk Density (g/cm^3)	Grain Density (g/cm^3)	Porosity (%)	Sonic Velocity (km/s)	Electrical Resistivity (ohm m)	Permeability (cm^2)
504B-4-1, 108-110	2.95	3.00	2.3	6.46	170	3.1×10^{-16}
6-2, 35-38	—	—	—	5.77	79.7	—
8-1, 63-65	2.94	3.00	2.9	6.14	98.2	4.0×10^{-16}
11-2, 76-78	2.90	2.98	4.0	5.94	108	—
12-1, 50-52	2.89	2.99	4.8	5.63	101	—
16-3, 134-136	2.93	2.99	3.0	5.95	80.4	—
17-1, 96-98	2.89	2.97	3.9	6.11	76.9	—
19-1, 101-103	2.84	2.92	4.2	5.87	145	3.3×10^{-16}
21-3, 123-125	—	—	—	5.92	161	—
24-2, 62-64	2.93	3.01	4.0	6.06	84.9	4.4×10^{-15}
32-1, 144-146	2.95	3.02	3.5	6.28	51.2	1.0×10^{-15}
32-2, 101-103	2.90	3.00	4.9	—	—	—
33-1, 130-132	2.92	2.99	3.6	6.09	50.1	—
33-2, 71-73	2.89	2.98	4.4	5.98	59.7	—
34-1, 10-12	2.95	3.01	3.3	5.95	56.3	—
34-1, 145-147	2.86	2.93	3.8	5.58	134	1.4×10^{-16}
34-2, 58-60	2.81	2.92	5.8	—	44.9	—
35-1, 115-117	2.83	2.95	6.5	5.91	42.2	—
36-2, 84-86	2.96	3.01	2.8	5.88	28.7	—
36-3, 15-17	2.88	2.97	4.8	5.90	29.6	—
37-1, 11-13	2.94	3.00	3.2	—	—	—
38-1, 83-85	2.98	3.02	1.6	6.37	155	1.7×10^{-15}
38-2, 109-111	2.97	3.04	3.7	—	—	—
39-1, 103-105	2.90	3.02	6.1	5.45	50.6	—
39-2, 117-119	2.94	2.98	2.3	6.21	74.9	—
40-1, 93-95	2.96	2.99	1.5	—	—	—
40-3, 35-37	2.92	2.97	2.6	6.27	99.6	—
40-4, 61-63	2.95	2.98	1.4	6.16	66.4	—
41-1, 112-114	2.95	2.98	1.7	6.30	58.1	—
41-2, 96-98	2.96	2.98	1.3	6.48	44.8	1.9×10^{-16}
41-3, 104-106	2.98	3.05	3.3	6.23	47.5	—
42-1, 31-33	2.88	2.98	5.3	5.70	33.4	—
42-2, 79-81	2.94	3.02	4.0	5.73	28.9	—
43-1, 9-11	2.96	3.04	3.8	6.16	32.0	—
43-2, 3-5	3.02	3.06	1.8	6.23	52.6	—
44-1, 79-81	2.96	3.03	3.6	6.10	42.3	—
45-1, 9-11	2.88	3.01	6.7	5.52	37.7	—
46-1, 74-76	3.00	3.04	2.2	6.28	79.7	—
47-3, 7-9	2.95	3.02	3.5	5.96	89.0	—
47-4, 98-100	2.97	3.03	2.9	6.24	51.9	—
48-2, 8-10	2.94	3.03	4.5	6.05	52.6	—
49-2, 58-60*	2.74	3.01	13.3	5.45	20.3	1.6×10^{-14}
50-1, 27-29	2.96	3.01	2.5	—	—	—
51-1, 105-107	2.95	3.01	2.8	6.25	30.2	—
52-1, 69-71	2.93	3.00	3.2	—	—	—
52-2, 29-31	2.94	3.01	3.5	5.99	30.9	—
54-1, 129-131	2.88	3.01	6.9	5.68	35.5	—
55-2, 24-26	2.89	3.01	6.3	5.72	58.5	—
56-2, 64-66	2.91	3.01	5.4	—	—	—
57-1, 39-41	2.90	3.02	6.1	5.76	38.1	—
57-2, 134-136	2.98	3.07	4.5	6.04	39.2	—
58-1, 110-112	2.94	3.05	5.5	6.14	35.4	2.8×10^{-16}
58-3, 109-111	2.96	3.02	3.4	6.09	36.4	4.7×10^{-15}
60-1, 65-67	2.97	3.04	3.5	6.15	60.7	—
61-2, 79-81	2.94	3.00	3.3	6.18	53.1	—
62-1, 106-108	2.91	2.97	2.9	—	—	—
63-2, 130-132	2.95	3.01	3.0	6.07	—	—
63-4, 77-79	2.95	3.01	2.7	5.96	47.5	—
64-2, 63-65	2.98	3.03	2.5	—	27.2	—
64-4, 2-4	2.94	3.01	3.3	5.93	34.4	—
65-1, 57-59	2.98	3.04	3.0	6.04	40.3	—
66-2, 84-86	2.99	3.05	2.7	6.12	44.8	1.0×10^{-15}
68-1, 0-2	2.84	2.98	7.1	—	—	—
69-1, 54-56	2.95	3.08	6.0	5.91	29.5	9.1×10^{-14}
70-1, 19-21*	2.77	3.03	12.8	4.60	14.5	—
70-2, 22-24	2.94	3.04	4.9	6.24	38.5	—

* Basalt breccia.

Table 2. Average physical properties.

Physical Properties	Hole 504B (this study)	Leg 37[a]	Legs 51, 52, 53[b]
Wet-bulk density (g/cm^3)	2.93 ± 0.05 (N = 64)	2.80 ± 0.08 (N = 101)	2.79 ± 0.13 (N = 185)
Grain density (g/cm^3)	3.01 ± 0.03 (N = 64)	2.95 ± 0.05 (N = 85)	2.91 ± 0.04 (N = 104)
Porosity (%)	4.1 ± 2.2 (N = 64)	7.8 ± 4.1 (N = 85)	8.4 ± 5.5 (N = 104)
Sonic velocity (km/s)	5.99 ± 0.31 (N = 55)	5.94 ± 0.34[c] (N = 79)	5.48 ± 0.48 (N = 189)
Electrical resistivity (ohm m)[d]	46.3 (N = 56)	220 (N = 87)	120 (N = 48)
Fluid permeability (cm^2)[d]	4.7×10^{-16} (N = 13)	—	1.1×10^{-16}[e] (N = 16)

[a] Hyndman and Drury (1976).
[b] Hamano (1979).
[c] Measured at 0.5 Kbar.
[d] Geometric mean.
[e] Air permeability.

The wet-bulk density of 64 basalts ranges from 2.74 for a basalt breccia to 3.02 g/cm^3 for a low-porosity basalt; the mean is 2.93 ± 0.05 g/cm^3. This mean value is among the highest observed in oceanic basalts. The grain density of 64 basalts ranges from 2.92 for a basalt breccia to 3.08 g/cm^3; the mean is 3.01 ± 0.03 g/cm^3, and this value is also among the highest. The porosity of 64 basalts ranges from 1.3% for a massive basalt to 13.3% for a basalt breccia; the mean is 4.1 ± 2.2%. Basalts from this hole have lower porosity than those from other DSDP sites, as shown in Table 2.

The high grain density and low porosity, which are responsible for the high wet-bulk density, may reflect the freshness of these basalts. In fact, highly altered basalts have generally low bulk density (e.g., Christensen and Salisbury, 1973), and a relatively altered basalt from Hole 504B (504B-34-2, 58-60 cm) has the lowest grain density (2.92 g/cm^3) and relatively high porosity (5.8%).

The difference in grain density between the upper part of drilled basement (Cores 1-40) and the lower part (Cores 41-70) is observed in Figure 2 (see also Karato et al., this volume).

SONIC VELOCITY

The sonic (compressional-wave) velocity of 55 basalts was measured under atmospheric pressure by a standard pulse transmission method, using the mercury delay line at frequency of 1 MHz. The accuracy of the measurements was checked by repeated measurements and by using aluminum standards; it is about 1%.

Shipboard measurements showed the anisotropy in velocity to be about 2%; the shore-based measurements (reported here) were made only on the horizontal wave velocities.

The compressional-wave velocity ranges from 4.60 km/s for a basalt breccia to 6.48 km/s for a low-porosity basalt; the mean is 5.99 ± 0.31 km/s. This mean value of sonic velocity is higher than that of average DSDP basalts (Christensen and Salisbury, 1975) and that of basalts from older ocean floor (e.g., Hamano, 1979), but comparable to that of young oceanic basalts (e.g., Hyndman and Drury, 1976; Kirkpatrick, 1979; Karato, in press).

The velocity-density and velocity-porosity relations are shown in Figures 3 and 4, respectively; the scatter of data points is smaller in the velocity-porosity diagram, suggesting that the major factor controlling the sonic velocity of these basalts is porosity. The linear regression for the velocity-porosity relation yields

$$V_p(\text{km/s}) = (6.448 \pm 0.053) - (0.111 \pm 0.011)\,\phi\ (\%), \qquad (1)$$

where V_p is the sonic velocity and ϕ is the porosity.

This relation suggests that the basalts with zero porosity have a sonic velocity of about 6.45 km/s. Since the pressure (and the temperature) affects the sonic

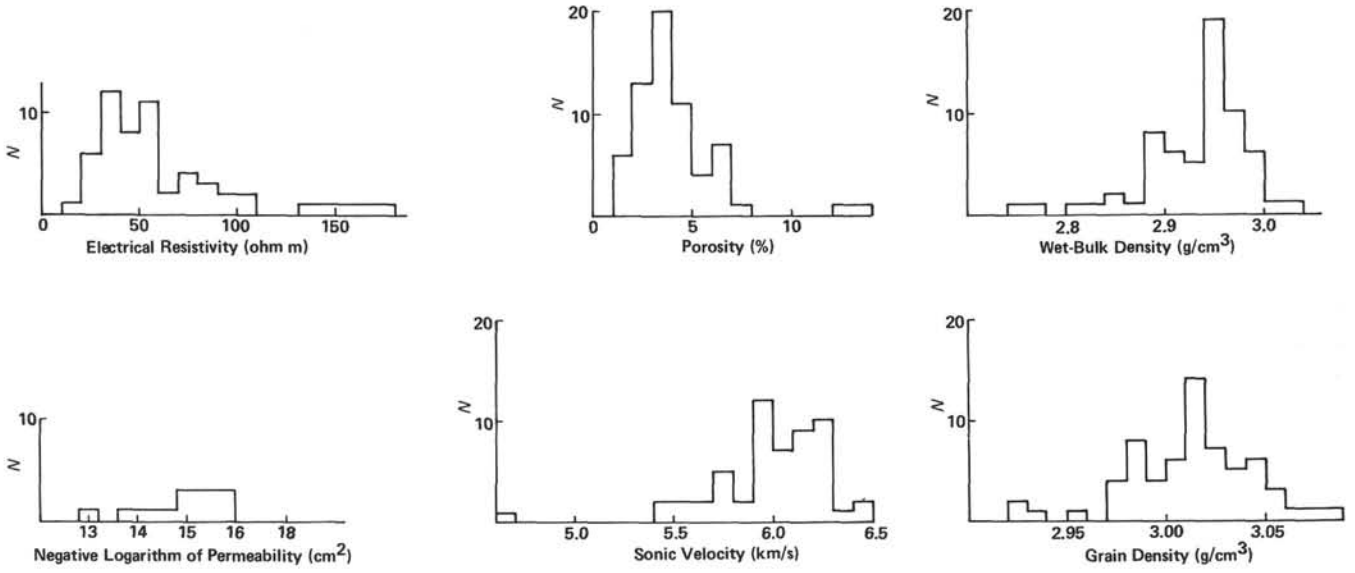

Figure 1. Histograms of physical properties.

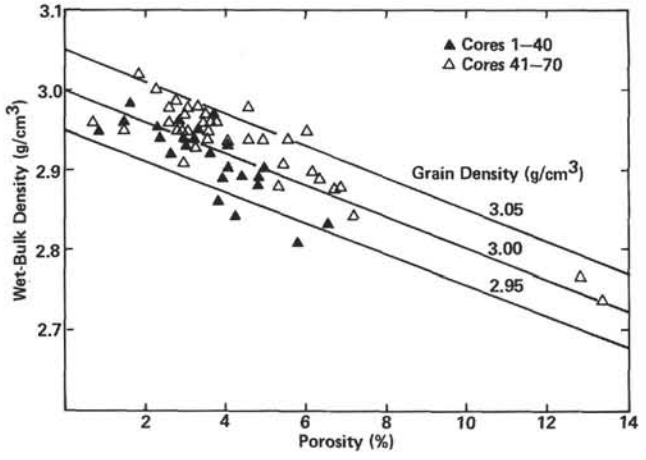

Figure 2. Relation of wet-bulk density and porosity. Solid lines are theoretical relations for grain densities of 3.05, 3.00, and 2.95 g/cm^3.

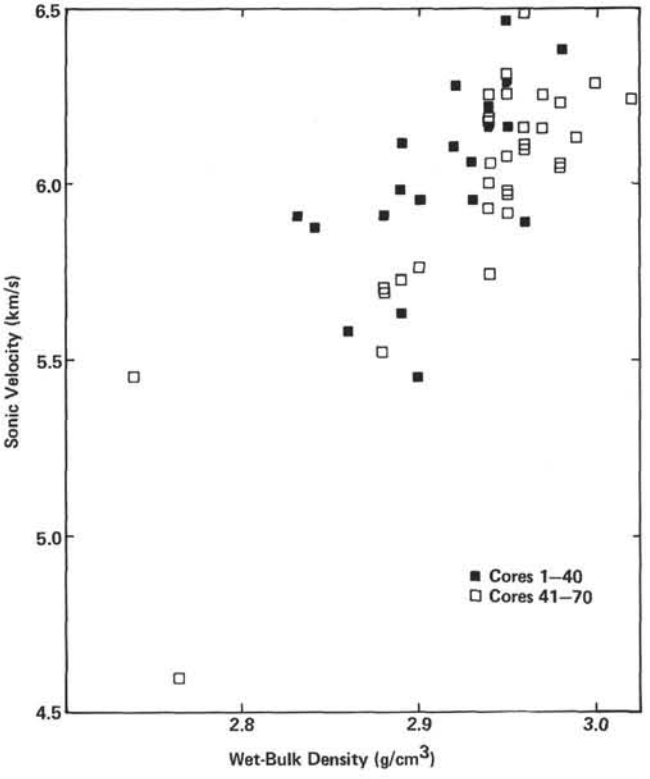

Figure 3. Relation of sonic velocity and wet-bulk density.

velocity mainly through the change in porosity, and the intrinsic pressure and temperature effect is minor in the shallow crust (Birch, 1961), this value of sonic velocity may be regarded as the upper limit of the sonic velocity of basalts with this composition.

Further, if the theoretical porosity–sonic-velocity relation of Toksöz et al. (1976) can be applied to these basalts, we could estimate the aspect ratio of pores (cracks) at about 0.1.

ELECTRICAL RESISTIVITY

The electrical resistivity of 56 basalts was measured at laboratory temperatures (22–25°C) and atmospheric pressure, using a 1-kHz AC bridge. Because the frequency dependence of electrical resistivity of oceanic basalts is small (Katsube et al., 1977), the results obtained here could be applied to the other frequencies used in resistivity logging. Platinum electrodes were attached to both ends of the cylindrical samples, and a rubber jacket was wrapped on the sample surface to prevent water evaporation. The resistivity of the sample can be determined within an error of 1%, but the reproducibility is only about 10%, probably because of the contact resistance at the electrodes. The electrical resistivity ranges from 14.5 ohm m for a basalt breccia to 170 ohm m for a low-porosity basalt; the geometric

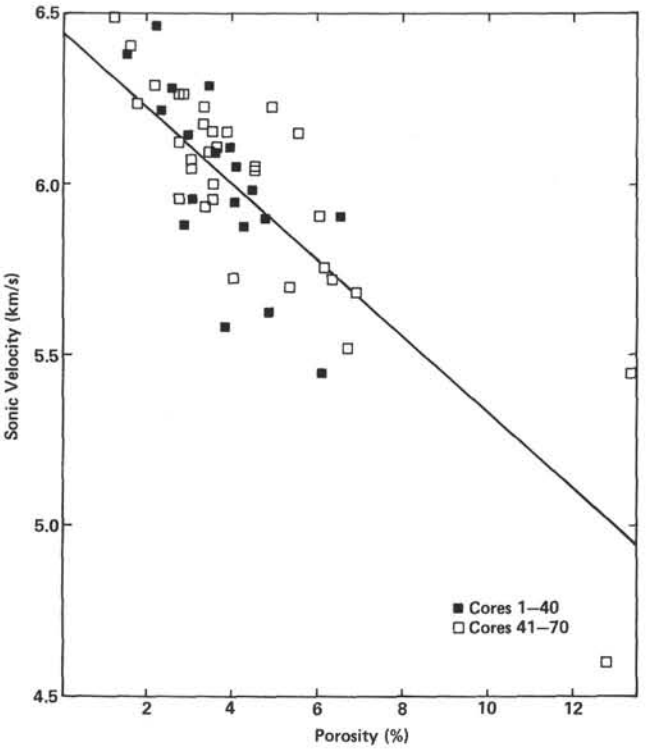

Figure 4. Relation of sonic velocity and porosity.

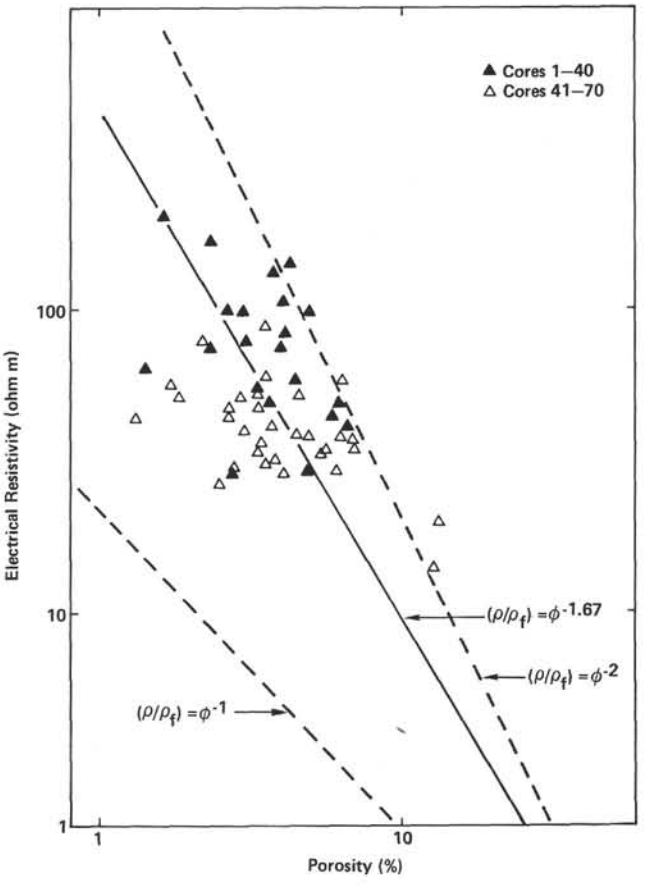

Figure 5. Relation of electrical resistivity and porosity.

mean is 46.3 ohm m. The electrical resistivity is plotted against porosity in Figure 5. The electrical resistivity of basalts from the upper part of this hole (Cores 1–40) is larger than that of the lower part (Cores 41–70), compared at the same porosity. Since the major petrological difference between the upper and the lower part of this hole is the difference in alteration (Honnorez et al., this volume), this could be attributed to the influence of secondary minerals on electrical resistivity. In fact, the temperature variation of electrical resistivity correlates with the degree of alteration (see the following), suggesting that alteration products could contribute to electrical conduction.

Although the data scatter is very large, Figure 5 shows a general trend of electrical resistivity decreasing with increasing porosity. Assuming Archie's law (Archie, 1942),

$$\varrho/\varrho_f = \phi^{-q}, \qquad (2)$$

where ϱ is the resistivity of sea-water-saturated rock, ϱ_f is the resistivity of sea water (0.2 ohm m), ϕ is the porosity, and q is a constant; the constant q is estimated at 1.67 ± 0.27.

The constant q in Archie's law may be related to the connectivity, and in turn to the shape of pores (e.g., Brace et al., 1965; Shankland and Waff, 1975), if the electrical conduction occurs mainly through pore fluids. The value of q obtained here (1.67) is less than 2, suggesting that the pores responsible for electrical conduction may be relatively flat. The validity of this conclusion, however, depends on the mechanism of electrical conduction and on the nature of porosity measured by the present method. If clay minerals at the surfaces of pores contribute to electrical conduction, as suggested by the temperature-variation data (see below), ϱ_f in equation (2) should be replaced with a smaller value; therefore, q would be larger than the value estimated above.

Porosity measured by the present method may include that due to isolated pores. On the other hand, only connected pores are responsible for electrical conduction. To discuss the pore shape, we must examine the relation between connected-pore porosity and resistivity. Because measured values of porosity represent the upper limit of the connected-pore porosity, the value of q estimated above is the upper limit of the actual value.

Although it is difficult to estimate these effects quantitatively, because these two factors affect the estimated value of q in the opposite sense, the above-cited value of q may be near the actual value.

The temperature variation of electrical resistivity was measured for 3 basalts, at temperatures from laboratory temperature to about 80°C. Measurements were made at both increasing and decreasing temperatures in a thermostat, and no hysteresis was found, showing that little water had evaporated during measurements. The

results are shown in Figure 6. The activation energy of electrical conduction was estimated by assuming the following relation:

$$\varrho = \varrho_0 \exp(E^*/RT)\, \phi^{-q}, \quad (3)$$

where ϱ_0 is a constant, E^* is the activation energy, and R and T have their usual meanings. The results are shown in Figure 6. In this figure, the temperature variation of electrical resistivity of sea water (e.g., Horibe, 1970) is also shown. The activation energy of a fresh basalt (504B-38-1, 83–85 cm) is very close to that of sea water, but those of a basalt breccia containing a large amount of smectite (504B-49-2, 58–60 cm) and of a slightly altered basalt (504B-60-1, 65–67 cm) are significantly larger than that of sea water. This suggests that alteration products in pores may play significant roles in electrical conduction.

FLUID PERMEABILITY

The permeability of sea water of 13 basalts was measured by a standard constant-head-pressure method at laboratory temperatures. A schematic diagram of the equipment is shown in Figure 7. Although the use of lesser-viscosity fluid, such as air (e.g., Hamano, 1979), could reduce the measurement time, we used the sea water itself, because the interaction of sea water with clay minerals in pores could be significant for fluid flow (Amyx et al., 1960). Measurements of permeability were made by applying a constant head pressure p of about 20 to 70 bar, which was kept constant within 0.5% during a run, under about 50- to 150-bar confining pressure. The volume of sea water Q passed through a sample in a given time interval Δt was measured, and the permeability k of the sample was calculated by Darcy's law as

$$k = \frac{Q}{\Delta t}\frac{\eta}{p}\frac{L}{A}, \quad (4)$$

where η is the viscosity of sea water (0.01 poise), L is the length of the sample, and A is its cross-sectional area. Measurements of volume flux of sea water were made for three time intervals, and the mean of these values was used for the permeability calculation.

The accuracy of each measurement was about 20%, but the reproducibility was only 50% or less. Plugging of pores by small particles may cause large fluctuations and result in large errors, because pore width (~0.03 μm; see below) is much smaller than the mesh dimension (0.46 μm) of the line filter.

The validity of Darcy's law (the linearity of the relation between head pressure and flow rate) was tested by measuring flow rates for several values of head pressures. The examples shown in Figure 8 show the linear relation within the experimental error.

The effect of confining pressure was examined for Sample 504B-58-3, 112–114 cm by varying confining pressure at constant head pressure (23 bar). The result is shown in Figure 9. At confining pressures up to about 50 bar, permeability decreases significantly with increases in confining pressure. At larger confining pressures, pressure effects on permeability are small. The large effects of confining pressure at low pressures could be attributed to the closure of weak paths (e.g., sample/rubber-sleeve boundary).

Considering the results of these two tests, the measurements of permeability were made mainly at about 70-bar head pressure and 150-bar confining pressure.

The permeability of basalts ranges from 1.4×10^{-16} to 9.1×10^{-14} cm^2; the geometric mean is 4.7×10^{-16} cm^2. Although these values compare well with those of fresh basalts from Hole 418A (Johnson, 1979), they are significantly lower than the large-scale permeability of oceanic crusts (10^{-11} to 10^{-10} cm^2) estimated from heat-flow data and the hydraulic impedance of sediment layers (Anderson et al., 1977; Karato and Becker, in press).

Permeability is plotted against porosity in Figure 10 and against resistivity in Figure 11. Although the data scatter is very large, the general trends are that the permeability increases with increase of porosity and also with decrease of electrical resistivity. Based on these plots, we were able to estimate the pore size using a model of fluid flow and electrical conduction in a porous medium.

Hubbert (1956; see also Brace, 1977) derived a relation between the electrical resistivity and the permeability of a fluid-saturated rock as

$$k = (m^2/k_0)\, F^{-2}\, \phi^{-1}, \quad (5)$$

where k is permeability, k_0 is a shape factor which can vary between 2 and 3, and ϕ is porosity. Here m is the

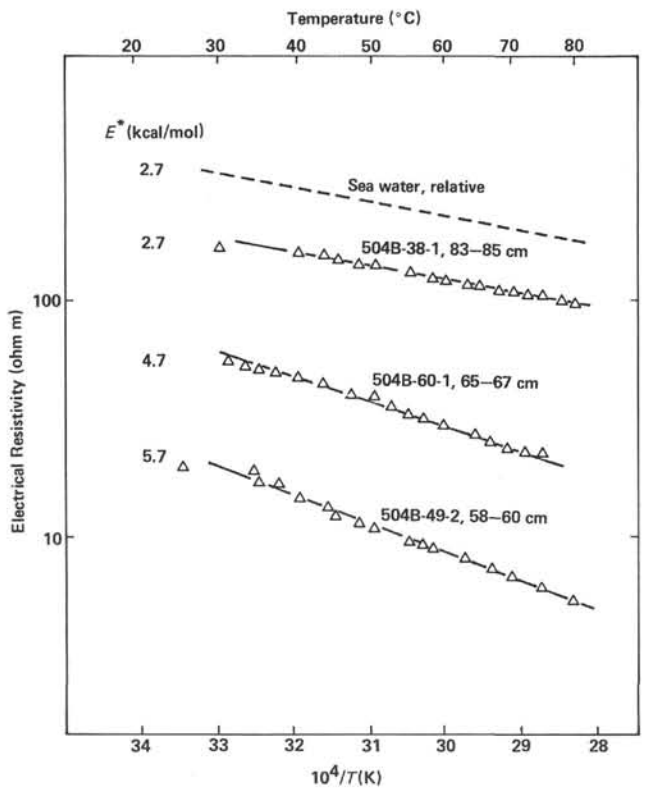

Figure 6. Temperature variation of electrical resistivity.

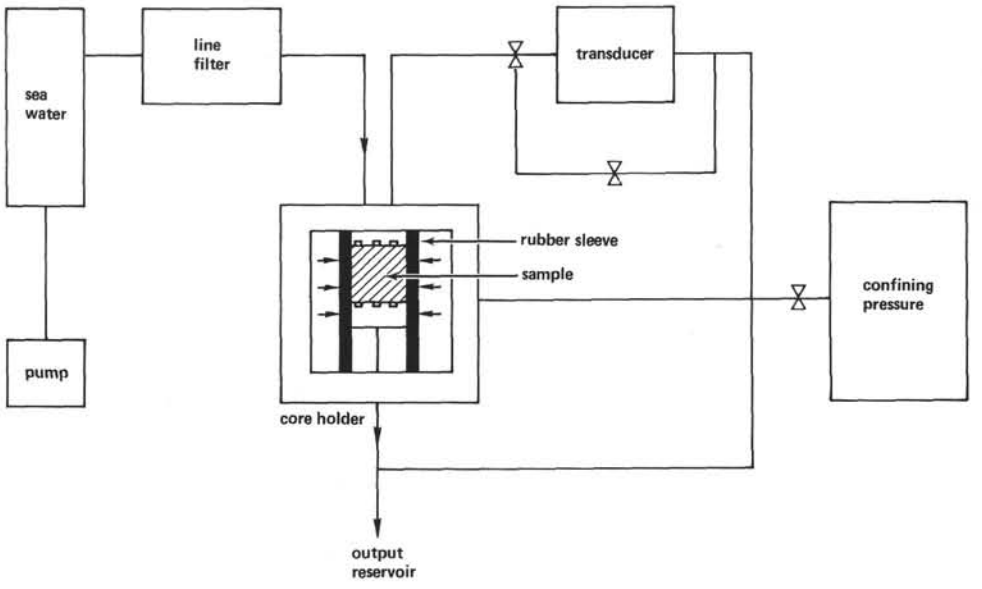

Figure 7. Schematic diagram of the permeability test apparatus.

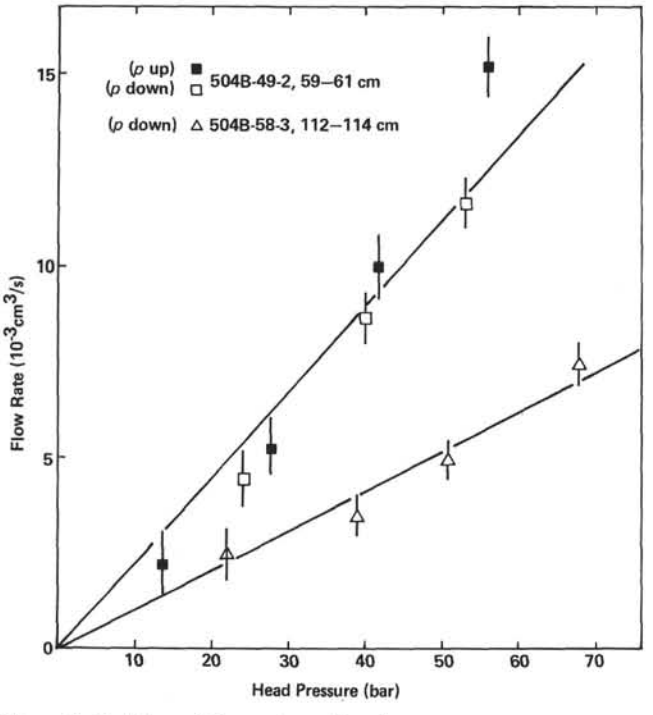

Figure 8. Relation of flow rate and head pressure.

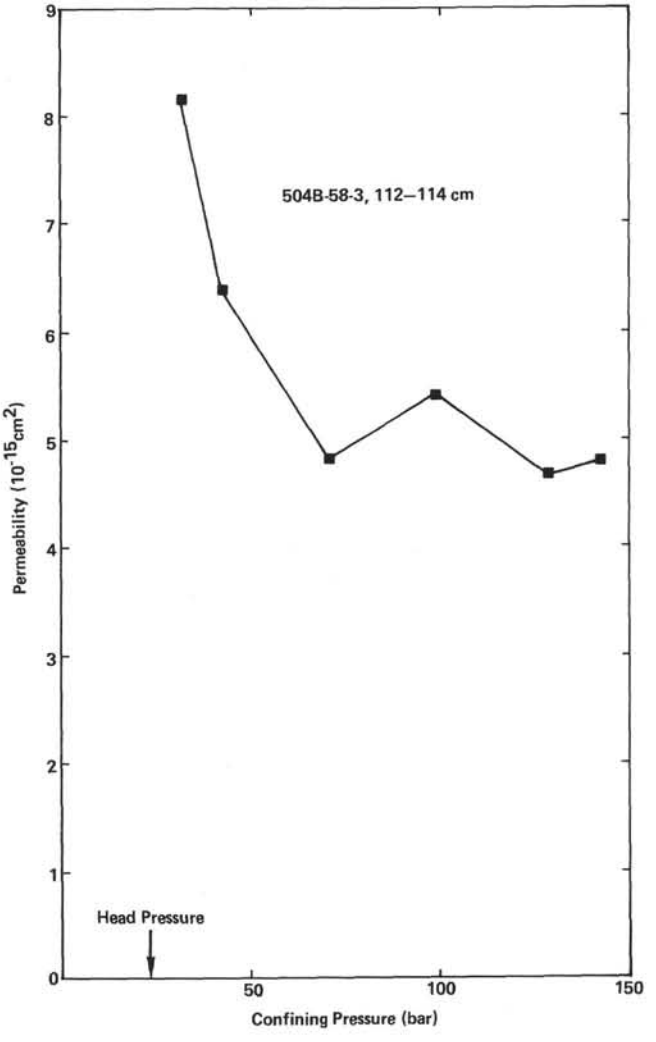

Figure 9. Relation of permeability and confining pressure.

hydraulic radius, which is the volume of the interconnected pores divided by their surface area. F is the formation factor, the ratio of the resistivity of fluid-saturated rock to the resistivity of fluid alone (ϱ/ϱ_f).

Combining equations (2) and (5), and substituting the value for q obtained earlier from equation (2), we have

$$k = (m^2/k_0)\,\phi^{2q-1} \quad (6)$$

$$= (m^2/k_0)\,\phi^{2.34} \quad (6')$$

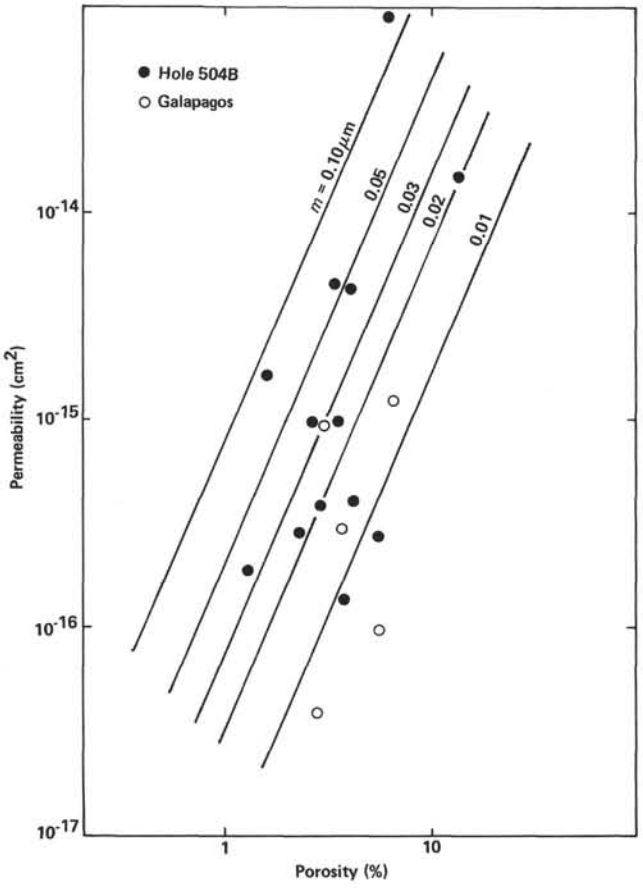

Figure 10. Relation of permeability and porosity. Solid lines show theoretical relations according to equation (6′) for various values of hydraulic radius m.

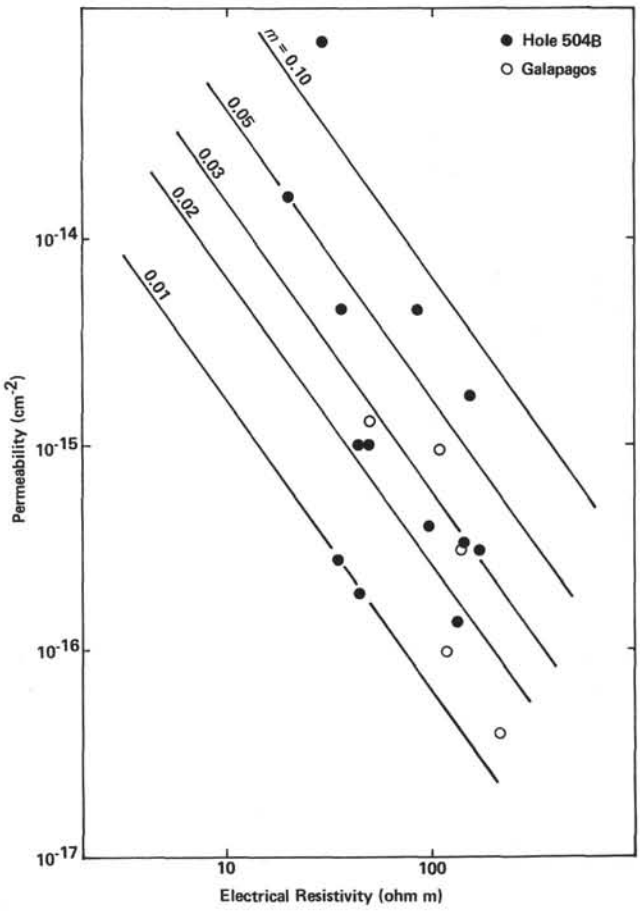

Figure 11. Relation of permeability and electrical resistivity. Solid lines show theoretical relations according to equation (7′) for various values of hydraulic radius m.

or

$$k = (m^2/k_0)\,(\varrho/\varrho_f)^{\frac{1-2q}{q}} \qquad (7)$$

$$= (m^2/k_0)\,(\varrho/\varrho_f)^{-1.40} \qquad (7')$$

Relations (6′) and (7′) for various values of m (for $k_0 = 2.5$) are shown in Figures 10 and 11. From these relations, we can estimate the hydraulic radius (pore radius) at 0.01 to 0.1 μm. These values are significantly smaller than the pore size observed in thin sections (>10 μm). These results therefore suggest that the large pores may be isolated or interconnected by small-radius pores, and the latter may determine the permeability of a rock specimen.

Further, Figure 10 suggests that the hydraulic radius m may increase with increasing porosity. In the following discussion, however, this possible dependence of m on porosity will be ignored, because the accuracy of the data is not sufficient to constrain the porosity of dependence of m quantitatively.

DISCUSSION

In this section, I discuss the physical state of the oceanic crust at Site 504, based on both laboratory measurements of physical properties and geophysical field measurements.

First, I will summarize the results of this study: laboratory measurements show that the major factor controlling the variation of physical properties of oceanic basalts from Hole 504B is their porosity. Temperature affects the electrical resistivity through the temperature dependence on resistivity of pore fluid and/or clay minerals; however, the temperature dependence of sonic velocity (Birch, 1966) and permeability (Amyx et al., 1960) are negligible in the crust. Further, the effect of pressure on these physical properties is mainly the effect of pressure on porosity (e.g., Birch, 1961; Brace et al., 1965; Brace et al., 1968); therefore, if we can estimate the porosity and temperature in the oceanic crust we could estimate the physical properties of crust by the laboratory data, when the relation between small-scale (laboratory measurements) and large-scale (field geophysical measurements) physical properties is known.

In the laboratory, the sonic velocity is measured by using a 1-MHz wave (i.e., wave length ~ 0.5 cm); on the other hand, seismic experiments use an approximately 10-Hz wave (i.e., wave length ~ 500 m); therefore, the sonic velocity measured by seismic experiments may include the effect of large-scale pores (up to the order of 100 m). On the other hand, sonic velocity measured in the laboratory includes only the effect of small-scale pores (less than millimeter size). Theories of sonic veloc-

ities in porous media (e.g., Toksöz et al., 1976) suggest that sonic velocities depend on the aspect ratio of pores, as well as on porosity. This implies that the velocity–porosity relation obtained by laboratory measurements according to equation (1) can be applied to field measurements only if the aspect ratio of pores is similar between small-scale (millimeter order) and large-scale (100-m order) pores. Although there is no *a priori* guarantee that this similarity holds, it is encouraging that the combination of sonic velocity and porosity logs (see Cann and Von Herzen, this volume) suggests that the velocity–porosity relation obtained in the laboratory could be applied to large-scale phenomena.

The situation is similar for electrical resistivity. Theoretical studies on electrical conduction in fluid-saturated media show that electrical resistivity depends not only on porosity, but also on the connectivity of pores (e.g., Shankland and Waff, 1975); therefore, laboratory data can be applied to larger-scale phenomena only if the pore geometry of small-scale and large-scale pores is similar. The approximate coincidence of porosities estimated from the resistivity log using Archie's law and from the porosity log (Cann and Von Herzen, this volume) could indicate that this similarity in pore geometry may hold.

For the permeability, however, there is no direct relation between small-scale and large-scale phenomena. Equations (5) and (6) or (7) show that permeability depends explicitly on hydraulic radius (pore width). Because the pore size in laboratory samples may be much smaller than that of large-scale pores in ocean crust, the permeability of the ocean crust may be much larger than that of laboratory samples, even if their porosity and pore geometry (i.e., the connectivity of pores) are the same. In fact, the packer measurement of fluid permeability at Hole 504B (Zoback and Anderson, this volume) yields a permeability of about 10^{-10} cm^2, which is about 10^3 to 10^4 times as much as the permeability estimated by the laboratory measurements, suggesting that the hydraulic radius of the oceanic crust is about 10 to 10^2 times as much as that of laboratory samples.

These arguments suggest that the velocity–porosity (1) and resistivity–porosity (and temperature) (3) relations could be applied to large-scale phenomena; thus, they could be used to reveal the physical structure of the oceanic crust.

On the other hand, laboratory data of permeability cannot be applied directly to large-scale phenomena. To bridge the gap between permeability of laboratory samples and ocean crust, we assume that the porosity dependence of permeability is the same, and that the only difference is their hydraulic radius. This assumption may be rationalized because electrical-resistivity studies show the similarity in pore geometry of laboratory samples and ocean crust. The hydraulic radius of large-scale pores in ocean crust is estimated by comparing the experimental equation (6′) with the packer experiments made at Hole 504B (Zoback and Anderson, this volume); for simplicity, this radius is assumed to be independent of depth. The variation of permeability with depth is assumed to be due to variation of porosity.

The depth variation of porosity is estimated by using equation (1) and observed velocity distribution (Stephen, this volume). Within the depth range of about 0 to 1 km below top of basement, seismic velocity is significantly smaller than the sonic velocity of laboratory samples, and it increases rapidly with depth. This suggests that large-scale pores (scales larger than laboratory samples) are abundant in this depth interval, and that large-scale porosity decreases rapidly with increasing depth. The estimated variation of porosity with depth is shown in Figure 12, together with the seismic-velocity distribution and other estimated physical properties. At about 2.5 km depth, the estimated porosity becomes essentially zero. Since equation (1) suggests that the upper limit of the sonic velocity of basalts is about 6.45 km/s, the layer below 2.5 km may be composed of rocks with higher sonic velocity than basalts (e.g., gabbro).

Using this porosity distribution, I estimate variations of electrical resistivity and permeability with depth from equations (3) and (6′). In the resistivity estimation, a conductive temperature profile is assumed (Fig. 12; see also Becker et al., this volume), and the temperature variation of resistivity of pore fluid is assumed to be equal to that of sea water.

Corresponding to the decrease of porosity with depth, the electrical resistivity and the permeability of the crust increase and decrease, respectively, with increasing depth. Of particular interest here is the distribution of permeability, which is related to the nature of hydrothermal circulation. Figure 12 shows that the permeability decreases with increasing depth at a rate of about 10^{-2}/km, or the depth variation of permeability may be approximately given by

$$k = k_0'' \exp(-z/z_0) \tag{8}$$

where k is the permeability (cm^2), z is the depth (km), $k_0'' \simeq 2 \times 10^{-10}$ cm^2, and $z_0 \simeq 0.3$ km. The permeability of the crust at Site 504 becomes essentially zero at depths below 2 to 3 km.

It is interesting that the rapid decrease of permeability with increasing depth suggested above is consistent with the results of numerical experiments by Green (1980), which suggest that the depth of fluid penetration is limited to the upper part of the ocean crust (at the Galapagos Rift).

ACKNOWLEDGMENTS

I wish to express my appreciation for the opportunity to participate on Leg 70 of the Deep Sea Drilling Project. I thank Jim Pine for the gravimetric measurements made aboard *Glomar Challenger;* Rikio Numajiri and Hiroshi Morishima for their assistance in the permeability measurements; Dick Von Herzen, Yozo Hamano, and Toshio Furuta for discussion; Naoyuki Fujii and Kei Kurita for reviewing the manuscript; and Sayuri Washida for typing the manuscript.

REFERENCES

Amyx, J. W., Bass, D. M., Jr., and Whiting, R. L., 1960. *Petroleum Reservoir Engineering:* New York (McGraw-Hill).

Anderson, R. N., Langseth, M. G., and Sclater, J. G., 1977. The mechanism of heat transfer through the floor of the Indian Ocean. *J. Geophys. Res.*, 82:3391–3409.

Archie, G. E., 1942. The electrical resistivity log as an aid in determining reservoir characteristics. *J. Petrol. Technol.*, 5:1–8.

Birch, F., 1961. The velocity of compressional waves in rocks to 10 Kbar, 2. *J. Geophys. Res.*, 66:2199–2224.

_____, 1966. Compressibility; elastic constants. *In* Clark, S. P., Jr. (Ed.), *Handbook of Physical Constants:* New York (Geol. Soc. Am.), pp. 97–173.

Brace, W. F., 1977. Permeability from resistivity and pore shape. *J. Geophys. Res.*, 82:3343–3349.

Brace, W. F., Orange, A. S., and Madden, T. R., 1965. The effect of pressure on the electrical resistivity of water-saturated crystalline rocks. *J. Geophys. Res.*, 70:5669–5678.

Brace, W. F., Walsh, J. B., and Frangos, W. T., 1968. Permeability of granite under high pressure. *J. Geophys. Res.*, 73:2225–2236.

Christensen, N. I., and Salisbury, M. H., 1973. Velocities, elastic moduli and weathering-age relations for Pacific layer 2 basalts. *Earth Planet. Sci. Lett.*, 19:461–470.

_____, 1975. Structure and constitution of the lower oceanic crust. *Rev. Geophys. Space Phys.*, 13:57–86.

Ewing, J., and Houtz, R., 1979. Acoustic stratigraphy and structure of the oceanic crust. *In* Talwani, M., Harrison, C. G., and Hayes, D. E. (Eds.), *Deep Drilling Results in the Atlantic Ocean: Ocean Crust:* Washington (Am. Geophys. Union), pp. 1–14.

Green, K. E., 1980. Geothermal processes at the Galapagos spreading center [Ph.D. dissert.]. Massachusetts Institute of Technology/ Woods Hole Oceanographic Institution.

Hamano, Y., 1980. Physical properties of basalts from Holes 417D and 418A. *In* Donnelly, T., Francheteau, J., Bryan, W., Robinson, P., Flower, M., Salisbury, M., et al., *Init. Repts. DSDP*, 51, 52, 53, Pt. 2: Washington (U.S. Govt. Printing Office), 1457–1466.

Horibe, S., 1970. Sea water as a solution. *In* Horibe, S. (Ed.), *Chemistry of Sea Water:* Tokyo (Tokai Univ. Press), pp. 26–45. [in Japanese]

Hubbert, M. K., 1956. Darcy's law and the field equations of the flow of underground fluids. *Trans. AIME*, 207:222–239.

Hyndman, R. D., and Drury, M. J., 1976. The physical properties of oceanic basement rocks from deep drilling on the Mid-Atlantic Ridge. *J. Geophys. Res.*, 81:4042–4052.

Johnson, D. M., 1980. Fluid permeability of oceanic basalts. *In* Donnelly, T., Francheteau, J., Bryan, W., Robinson, P., Flower, M., Salisbury, M., et al., *Init. Repts. DSDP*, 51, 52, 53, Pt. 2: Washington (U.S. Govt. Printing Office), 1473–1477.

Karato, S., in press. Physical properties of basalts from Galapagos, Leg 70. *In* Von Herzen, R. P., Honnorez, J., et al., *Init. Repts. DSDP*, 70: Washington (U.S. Govt. Printing Office).

Karato, S., and Becker, K., in press. Physical properties of sediments from Galapagos and their implications for hydrothermal circulation. *In* Von Herzen, R. P., Honnorez, J., et al., *Init. Repts. DSDP*, 70: Washington (U.S. Govt. Printing Office).

Katsube, T. J., Frechette, J., and Collett, L. S., 1977. Preliminary electrical measurements of core samples, DSDP Leg 37. *In* Aumento, F., Melson, W. G., et al., *Init. Repts. DSDP*, 37: Washington (U.S. Govt. Printing Office), 417–421.

Kirkpatrick, R. J., 1979. The physical state of the oceanic crust: results of downhole geophysical logging in the Mid-Atlantic Ridge at 23°N. *J. Geophys. Res.*, 84:178–188.

Lister, C. R. B., 1972. On the thermal balance of a mid-oceanic ridge. *Geophys. J. Royal Astr. Soc.*, 26:515–535.

Shankland, T. J., and Waff, H. S., 1975. Conductivity in fluid-bearing rocks. *J. Geophys. Res.*, 79:4863–4868.

Toksöz, N., Cheng, C. H., and Timur, A., 1976. Velocities of seismic waves in porous rocks. *Geophysics*, 41:621–645.

Williams, D. L., Von Herzen, R. P., Sclater, J. G., and Anderson, R. N., 1974. The Galapagos spreading centre: lithospheric cooling and hydrothermal circulation. *Geophys. J. Royal Astr. Soc.*, 38: 587–608.

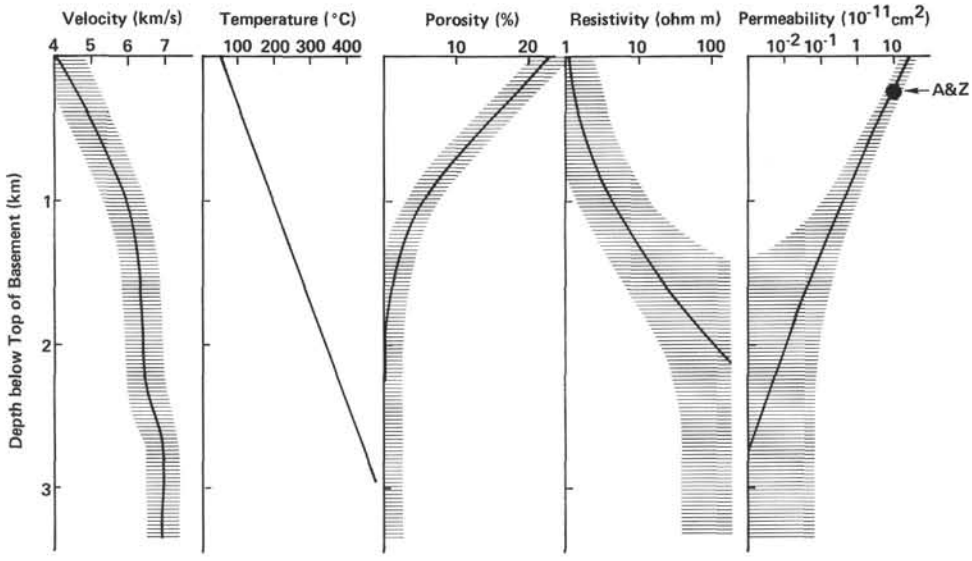

Figure 12. Depth variation of physical properties in ocean crust of the Costa Rica Rift (see text).